Measurement and Modeling of the Solubility of 9H-Carbazole in Sub- and Supercritical Propane

ARTICLE *in* JOURNAL OF CHEMICAL & ENGINEERING DATA · FEBRUARY 2011

Impact Factor: 2.04 · DOI: 10.1021/je100923d

4 AUTHORS, INCLUDING:

Fabiola Martínez
University of Castilla-La Mancha
32 PUBLICATIONS **825** CITATIONS
SEE PROFILE

Rafael Camarillo
University of Castilla-La Mancha
27 PUBLICATIONS **363** CITATIONS
SEE PROFILE

Jesusa Rincon
University of Castilla-La Mancha
48 PUBLICATIONS **515** CITATIONS
SEE PROFILE

JOURNAL OF CHEMICAL & ENGINEERING DATA

ARTICLE

pubs.acs.org/jced

Measurement and Modeling of the Solubility of 9*H*-Carbazole in Sub- and Supercritical Propane

Fabiola Martínez, Alicia Martín, Rafael Camarillo, and Jesusa Rincón*

Department of Chemical Engineering, Faculty of Environmental Sciences, Universidad de Castilla-La Mancha, Avda. Carlos III, s/n, 45071 Toledo, Spain

ABSTRACT: The solubility of 9*H*-carbazole in sub- and supercritical propane has been measured using a static view cell at pressures from (4.3 to 10.0) MPa and temperatures from (323 to 405) K. The mole fraction of 9*H*-carbazole varied from $4 \cdot 10^{-5}$ to $4 \cdot 10^{-4}$ over the experimental range studied. The solubility of 9*H*-carbazole in propane is 1 order of magnitude higher than that of 9*H*-carbazole in CO_2 for similar values of the reduced pressure and temperature, which highlights the excellent solvent properties of propane relative to CO_2 for the extraction of polyaromatic compounds. The experimental solubility data were correlated with the Peng−Robinson equation of state using six different sets of mixing rules for the estimation of the mixture parameters a_M and b_M. Good fits of the experimental results were obtained for all of the mixing rules tested, especially for those involving two adjustable parameters; the absolute average percentage deviation (AAPD) was 16.4 % for the best fit. In addition, the empirical equation of Chrastil was used to model the experimental solubility, and a similar AAPD (16.6 %) was obtained. In this case, because of the simplicity of the empirical model, three adjustable parameters were required for the adjustment. Both of the mathematical expressions evaluated (Peng−Robinson and Chrastil) can be used for the prediction of the solubility of 9*H*-carbazole in propane.

1. INTRODUCTION

Over the years, supercritical fluid (SCF) solvents have been used in a large number of extraction processes. In most studies, supercritical CO_2 has been the solvent of choice because of its relatively low critical temperature and pressure, high purity at low cost, and its ability to serve as an environmental friendly replacement for traditional organic solvents.

Among other extraction processes, supercritical fluid extraction (SFE) of polycyclic aromatic hydrocarbons (PAHs) has received much attention for its possible application to remove this type of compound from soils, spent catalysts, and sludges for either analytical or remediation purposes.[1−5] At present, it can be stated that SFE using carbon dioxide is a quite well established process that in the case of the food industry has been used commercially for more than 3 decades.

In contrast, there is another very interesting area of SCF technology in a later state of development. It deals with the use of the supercritical solvent in reactions where it may either actively participate in the reaction or function only as the solvent medium for reactants, catalysts, and products. Examples of both uses involving PAHs have been reported elsewhere.[6−9]

In current research, a common factor that is considered important for both SCF applications (extraction and reaction) is the need for a thorough understanding and knowledge of the solubility of the compounds of interest in the SCF. These are required for the design of the operation units and the development of the extraction or reaction models and are used as a first approach to establish the technical and economic viability of the SCF process.

Solubility data in supercritical CO_2 have been tabulated in the literature for a large number of aromatic substances.[10−14] However, solubility studies of these compounds in other solvents, while scarce, are necessary because for the above-mentioned reasons.[15−20]

Table 1. Molar Mass (M), Normal Boiling Temperature (T_{bp}), Melting Temperature (T_{mp}), Critical Temperature (T_c), Critical Pressure (P_c), and Acentric Factor ω for 9*H*-Carbazole and Propane

compound	M/g·mol^{-1}	T_{bp}/K	T_{mp}/K	T_c/K	P_c/MPa	ω
propane	44.09562[g]	231.06[a]	85.5[b]	369.825[c]	4.24766[a]	0.1518[d]
9*H*-carbazole	167.20660[g]	628.2[e]	—	901.8[f]	3.1309[f]	0.461[f]

[a] Value taken from ref 24. [b] Value taken from ref 25. [c] Value taken from ref 26. [d] Value taken from refs 27 and 28. [e] Value taken from ref 29. [f] Value taken from ref 30. [g] Value taken from ref 31.

In particular, we have not found any report on the solubility of 9*H*-carbazole in propane.

In this work, considering that the solvent properties of propane may be superior to those of CO_2 for 9*H*-carbazole[15,21,22] and also taking into account the low critical constants and large availability of this solvent, we measured the solubility of this heterocyclic aromatic compound in sub- and supercritical propane between (323 and 405) K at pressures in the range (4.3 to 10.0) MPa. We also compared the experimental solubility to that obtained using CO_2,[23] the SCF solvent most commonly used. In addition, the solubility data were modeled with the Peng−Robinson equation of state (using different sets of mixing rules for the calculation of the parameters a_M and b_M) and the empirical equation of Chrastil.

Special Issue: John M. Prausnitz Festschrift

Received: September 10, 2010
Accepted: January 13, 2011

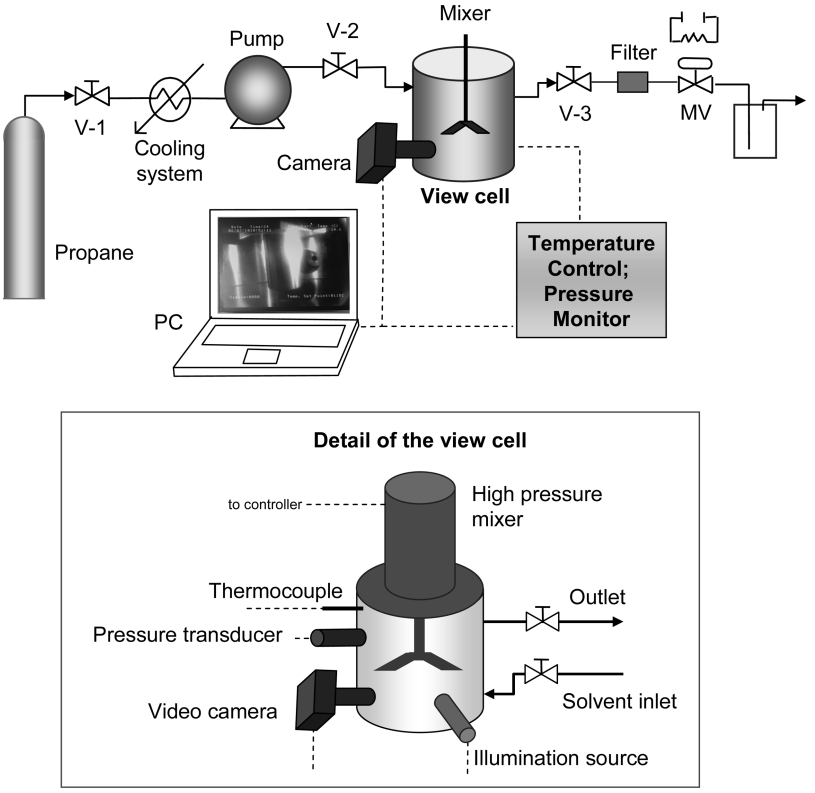

Figure 1. Layout of the experimental setup.

2. EXPERIMENTAL SECTION

2.1. Materials and Experimental Setup. Propane (mass fraction 0.995, Praxair) and 9*H*-carbazole (mass fraction 0.980, Aldrich) were employed without further purification. The main physical properties of 9*H*-carbazole and propane are shown in Table 1. The molar volumes of propane were obtained from NIST.[24] The vapor pressure of 9*H*-carbazole ($P^{vap}_{carbazole}$) was calculated using eq 1.[32]

$$\log_{10}(P^{vap}_{carbazole}/Pa) = 14.04 - \frac{5288.4}{T/K} \quad (1)$$

The solubility of 9*H*-carbazole in propane was measured using an experimental setup (R100CW) supplied by Thar Technologies, Inc. (Pittsburgh, PA), as shown in Figure 1. The setup consisted of a view cell (volume 0.1 L) with two sapphire windows mounted 90° apart for the observation and recording of the phase behavior inside the cell using a camera and an illumination source. It was equipped with a pressure transducer, a temperature controller (with embedded heaters), a high-pressure motor-driven mixer, and a pressure pump (P-50, Thar Technologies). A cooling system was used to cool the propane before it was pumped to the solubility determination equipment. The camera, which was connected to a PC, allowed the observation and recording of the phase behavior inside the cell under all of the pressure and temperature conditions tested.

For decompressing the system, a metering valve (labeled MV in Figure 1) with a heating device was used. A filter protected the metering valve against blockage due to solidification of 9*H*-carbazole during decompression.

2.2. Experimental Procedure. To obtain the static solubility data, a given amount of 9*H*-carbazole was placed inside the cell. After that, the cell was closed and heated to a given temperature by means of the embedded heaters and the temperature controller. Once the set temperature was reached, the mixer was switched on and the propane pumped into the cell. To determine the 9*H*-carbazole solubility, the pressure was increased (under isothermal conditions) in short intervals of (0.2 to 0.4) MPa until the point at which only one phase was observed through the sapphire window. Between intervals, the pressure was held for about 300 s before the next increase. The experiments were recorded on the PC connected to the camera. This allowed the subsequent viewing of the phase equilibrium images with their corresponding real-time pressure and temperature data. The solubility was determined from the amounts of 9*H*-carbazole and propane loaded into the cell. The reported solubility data are means of two replicated experiments.

The experimental pressure and temperature conditions used in each experiment are marked in Figure 2, where the regions for the liquid, vapor, and supercritical (SC) states of propane are also indicated. Dotted lines are also drawn in Figure 2 to indicate the quasi-isobars at which the temperature effect was investigated. In view of the fact that with the solubility measurement equipment described above (see section 2.1) it was extremely difficult to fix the exact pressure value at which the solute solubility would be determined prior to performing the experiment, pressure values differing by less than 0.2 MPa were considered to belong to the same isobar.

Finally, it should be mentioned that according to the manufacturer's specifications of the equipment, the standard uncertainty in the cell volume was 0.08 mL, and the possible pressure and temperature variations in the cell were in the ranges ± 0.2 MPa and ± 3 °C, respectively. On the other hand, the uncertainty associated with the propane density was 2.3 %, as estimated on the basis of three major influences: pressure and temperature effects on the density and the uncertainty in the reference data for

dx.doi.org/10.1021/je100923d |*J. Chem. Eng. Data* XXXX, XXX, 000–000

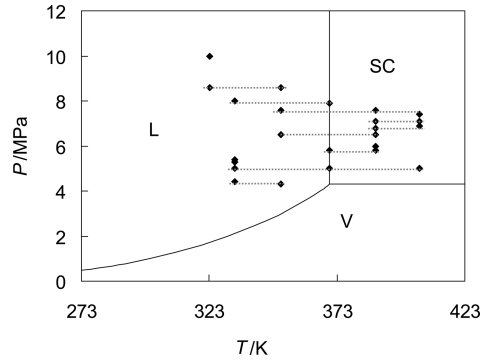

Figure 2. Experimental conditions and quasi-isobars marked on the phase diagram of propane.

the density.[33] According to the relationship between the mass and density of propane (i.e., $m_{propane} = \rho \cdot V$, in which ρ and V are the propane density and the volume of the cell, respectively), the relative combined standard uncertainty in the propane mass, $u_r(m_{propane})$, was 0.023 [i.e., $u_r(m_{propane}) = \Delta m_{propane}/m_{propane} = 0.023$]. The uncertainty in the mass of 9*H*-carbazole was 0.5 mg, according to the balance calibration certificate and the manufacturer recommendations. The standard uncertainties in the 9*H*-carbazole and propane molar masses[31] were (0.00553 and 0.00142) $g \cdot mol^{-1}$, respectively. Lastly, all of these uncertainty data and an error propagation analysis[34,35] allowed the uncertainty in the 9*H*-carbazole mole fraction to be estimated. The results obtained are shown Table 2. It can be observed that in all cases, the relative uncertainty in the mole fraction of 9*H*-carbazole, $u_r(y_2)$, is less than or equal to 0.066 [i.e., $u_r(y_2) = \Delta y_2/y_2 \leq 0.066$].

3. RESULTS AND DISCUSSION

Table 2 shows the solubility of 9*H*-carbazole in propane (expressed as the mole fraction of 9*H*-carbazole, y_2) obtained in the experiments carried out in this work. The y_2 values obtained are in the range from $4.5 \cdot 10^{-5}$ to $4.2 \cdot 10^{-4}$, which is equivalent to solubility values from (0.17 to 1.58) (mg of 9*H*-carbazol) · (g of propane)$^{-1}$. It can be observed that isothermal increases in pressure caused increases in the amount of 9*H*-carbazole that propane can solubilize. On the other hand, it may also be observed that at the higher pressures tested (above 6 MPa), isobaric increases in temperature led to increases in the solubility. However, at pressures below 6 MPa, although the trend continued (increasing solubility with isobarically increasing temperature), it was less pronounced. In regard to the solubility of 9*H*-carbazole around the critical point of propane, its variation with temperature and pressure was similar to that found over the whole region investigated, as can be inferred from the experimental data in Table 2.

As will be shown below, these results are closely related to the dependence on temperature and pressure of both the propane density and the 9*H*-carbazole vapor pressure, which are the main parameters influencing the solubility of the solute. It should be noticed that the effect of these variables (fluid density and solute vapor pressure) on solute solubility has been reported elsewhere for a number of systems.[36,37] In general, it has been found that the higher the fluid density, the larger its solvent power, and on the other hand, the higher the solute vapor pressure, the larger its solubility.

Table 2 shows not only the results obtained in the experiments but also the values of the density of propane and the vapor pressure of 9*H*-carbazole under the corresponding operation conditions. It can be observed that isothermal increases in pressure lead to increases in the density of propane, whereas isobaric increases in temperature cause decreases in this parameter. Likewise, it can be seen that the vapor pressure of 9*H*-carbazole increases exponentially with temperature. According to these observations, high values of pressure must favor increased solubility because of the higher values of the propane density. Nevertheless, high temperatures cause contrary effects on the main parameters affecting the solubility. Specifically, increasing the temperature on one hand results in a decrease in the density of propane (and its solvent power), a fact that has a negative effect on the solute solubility, and on the other hand causes an increase in the 9*H*-carbazole vapor pressure, which has a positive effect on the solubility.

Therefore, the increase in the 9*H*-carbazole solubility obtained by increasing the pressure at constant temperature can be explained by the effect of pressure on the density of propane. On the other hand, the variations of solubility attained by isobarically increasing the temperature should be attributed to the combined effect of temperature increase on the propane density and 9*H*-carbazole vapor pressure. Thus, for pressures below 6 MPa, a significant decrease of the propane density is observed at temperature values above the supercritical temperature of propane.[24] However, at pressures above 6 MPa, a softer decrease in the propane density relative to that observed below 6 MPa is associated with isobaric

Table 2. Experimental Data for the Solubility of 9*H*-Carbazole in Propane (y_2), the Density of Propane ($\rho_{propane}$), and the Vapor Pressure of 9*H*-Carbazole for the Different Operation Conditions Studied

T/K	P/MPa	y_2[a]	$u_r(y_2)$[b]	$\rho_{propane}$[c]/kg·m^{-3}	$P^{vap}_{carbazole}$[d]/MPa
323	8.6	$4.5 \cdot 10^{-5}$	0.066	477.3	$4.730 \cdot 10^{-9}$
	10.0	$5.1 \cdot 10^{-5}$	0.058	481.7	$4.730 \cdot 10^{-9}$
333	4.4	$4.8 \cdot 10^{-5}$	0.066	443.3	$1.466 \cdot 10^{-8}$
	5.0	$5.3 \cdot 10^{-5}$	0.061	446.3	$1.466 \cdot 10^{-8}$
	5.3	$5.8 \cdot 10^{-5}$	0.056	447.9	$1.466 \cdot 10^{-8}$
	5.4	$6.6 \cdot 10^{-5}$	0.050	448.4	$1.466 \cdot 10^{-8}$
	8.0	$8.6 \cdot 10^{-5}$	0.041	460.0	$1.466 \cdot 10^{-8}$
351	4.3	$1.0 \cdot 10^{-4}$	0.040	399.5	$9.545 \cdot 10^{-8}$
	6.5	$1.3 \cdot 10^{-4}$	0.034	418.4	$9.545 \cdot 10^{-8}$
	7.6	$1.6 \cdot 10^{-4}$	0.030	425.6	$9.545 \cdot 10^{-8}$
	8.6	$1.8 \cdot 10^{-4}$	0.029	431.2	$9.545 \cdot 10^{-8}$
370	5.0	$1.8 \cdot 10^{-4}$	0.032	335.2	$5.660 \cdot 10^{-7}$
	5.8	$1.8 \cdot 10^{-4}$	0.030	357.8	$5.660 \cdot 10^{-7}$
	7.9	$2.2 \cdot 10^{-4}$	0.028	385.7	$5.660 \cdot 10^{-7}$
388	5.8	$9.3 \cdot 10^{-5}$	0.067	227.4	$2.602 \cdot 10^{-6}$
	6.0	$1.6 \cdot 10^{-4}$	0.040	250.1	$2.602 \cdot 10^{-6}$
	6.5	$2.1 \cdot 10^{-4}$	0.032	288.1	$2.602 \cdot 10^{-6}$
	6.8	$2.5 \cdot 10^{-4}$	0.029	300.5	$2.602 \cdot 10^{-6}$
	7.1	$2.7 \cdot 10^{-4}$	0.028	313.0	$2.602 \cdot 10^{-6}$
	7.6	$3.1 \cdot 10^{-4}$	0.026	325.9	$2.602 \cdot 10^{-6}$
405	5.0	$2.0 \cdot 10^{-4}$	0.066	105.4	$9.706 \cdot 10^{-6}$
	6.9	$2.4 \cdot 10^{-4}$	0.035	207.0	$9.706 \cdot 10^{-6}$
	7.1	$3.7 \cdot 10^{-4}$	0.028	222.7	$9.706 \cdot 10^{-6}$
	7.4	$4.2 \cdot 10^{-4}$	0.026	242.0	$9.706 \cdot 10^{-6}$

[a] Mole fraction of 9*H*-carbazole. [b] Relative combined standard uncertainty in the 9*H*-carbazole mole fraction: $u_r(y_2) = \Delta y_2/y_2$. [c] Data taken from ref 24. [d] Data taken from ref 32.

dx.doi.org/10.1021/je100923d |*J. Chem. Eng. Data* XXXX, XXX, 000–000

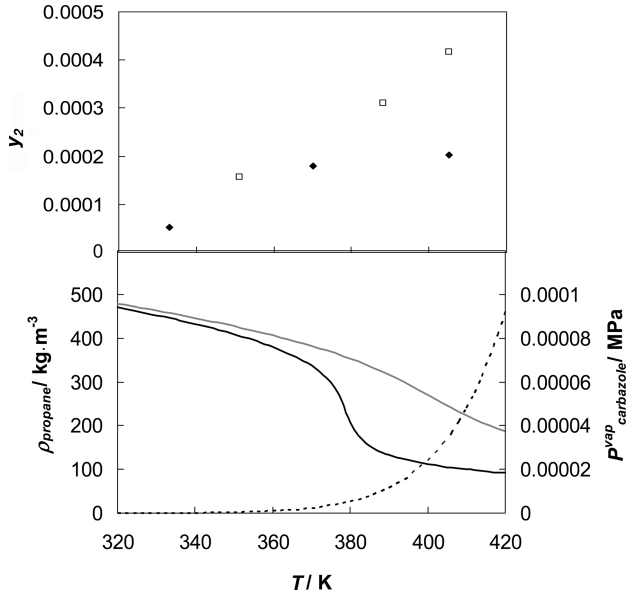

Figure 3. Experimental data for the solubility of 9*H*-carbazole in propane as a function of temperature together with the corresponding propane densities and 9*H*-carbazole vapor pressures. Mole fraction of 9*H*-carbazole in propane (y_2): ◆, P = 5.0 MPa; □, P = 7.5 MPa. Propane density ($\rho_{propane}$): black solid line, P = 5.0 MPa; gray solid line, P = 7.5 MPa; 9*H*-Carbazole vapor pressure ($P^{vap}_{carbazole}$): black dashed line.

Table 3. Comparison of the Solubilities of 9*H*-Carbazole (y_2) in Propane and CO_2

CO_2[a]					propane (this work)				
T_r[b]	T/K	P_r[c]	P/MPa	$10^5 \cdot y_2$	T_r[b]	T/K	P_r[c]	P/MPa	$10^5 \cdot y_2$
1.01	308	1.31	10.3	1.43	1.00	370	1.36	5.8	18.5
1.01	308	1.54	12.1	1.62	1.05	388	1.51	6.5	21.2

[a] Data taken from ref 23. [b] $T_r = T/T_c$. [c] $P_r = P/P_c$.

increases in temperature. As a result of this fact, increasing the temperature isobarically at pressures above 6 MPa causes the effect of the solute vapor pressure on the 9*H*-carbazole solubility to clearly dominate over that of the fluid density. As a consequence, the solubility of 9*H*-carbazole increases in a more pronounced way with isobaric increases in temperature at pressures above 6 MPa. These effects can be observed graphically in Figure 3, which shows the results for the solubility of 9*H*-carbazole as a function of temperature at constant values of pressure [concretely, (5.0 and 7.5) MPa] together with the corresponding values of the fluid density[24] and solute vapor pressure.[32]

In regard to the use of propane rather than supercritical CO_2 (the SCF solvent most commonly used), the results obtained in this work were compared to those reported by Goodarznia and Esmaeilzadeh.[23] Table 3 shows a comparison of the 9*H*-carbazole mole fractions in propane and CO_2 for similar values of the reduced temperature and pressure (T_r, P_r). Treatment of solubility data in this manner removes the effect of proximity to the critical point. It can be observed that in all cases the y_2 values in propane are 1 order of magnitude larger than those reported for CO_2. These observations are indicative of the excellent solvent properties of propane relative to supercritical CO_2 for the extraction of polyaromatic compounds.

3.1. Data Correlation: Peng−Robinson Equation of State.

The fundamental relationship expressed by eq 2 can be used to calculate the solubility of a solid solute in equilibrium with a fluid at high pressure:

$$y_2 = \frac{P_2^{vap}}{P} \cdot \frac{1}{\varphi_2^F} \cdot \exp\left(\frac{v_2^{sat} \cdot (P - P_2^{vap})}{R \cdot T}\right) \quad (2)$$

where y_2 is the mole fraction of the solute, P_2^{vap} and v_2^{sat} denote its saturated vapor pressure and solid-state molar volume, respectively, P and T are the equilibrium pressure and temperature, respectively, R is the universal gas constant, and φ_2^F is the fugacity coefficient of the fluid phase (which is indicative of the nonideal behavior of the fluid phase). As indicated above, the saturated vapor pressure of 9*H*-carbazole was estimated using eq 1, and a value of $1.51 \cdot 10^{-4}$ m$^3 \cdot$mol^{-1} was used for the solid molar volume.[38] For the calculation of the fugacity coefficient φ_2^F, cubic equations of state are often used, as these semiempirical equations offer simplicity and accuracy. Among the most commonly used cubic equations of state is the one proposed by Peng and Robinson, which involves the use of two parameters (a and b for pure components).[39]

To extend the Peng−Robinson equation of state to mixtures of components, the mixture parameters (a_M and b_M) are adopted. These mixture parameters involve the pure-component parameters a_i and b_i and the mole fraction y_i of each component i in the mixture and can be estimated from eqs 3:

$$\begin{aligned} a_M &= \sum_i \sum_j y_i \cdot y_j \cdot a_{ij} \\ b_M &= \sum_i \sum_j y_i \cdot y_j \cdot b_{ij} \end{aligned} \quad (3)$$

For the calculation of a_{ij} and b_{ij}, different sets of mixing rules can be used. In this work, six different sets of mixing rules (summarized in Table 4) were tested for the estimation of a_{ij} and b_{ij} in order to improve the correlation of the experimental solubilities. These mixing rules involve the calculation of adjustable parameters (k_{12}, δ_{12}, and k_{21}). The Newton method was used to obtain the optimal values of the adjustable parameters by comparing the values of the mole fractions calculated with the Peng−Robinson equation (y_2^{calcd}) to the experimental ones (y_2).[15] The objective function (OBF) given by eq 4 was minimized for each mixing rule tested:

$$OBF = \sum_{i=1}^{n} \frac{\left| y_{2,i} - y_{2,i}^{calcd} \right|}{y_{2,i}} \quad (4)$$

In this equation, n is the total number of experimental 9*H*-carbazole mole fractions.

Likewise, in order to evaluate which of the mixing rules allowed the best correlation of the experimental solubilities of 9*H*-carbazole in propane over the range of temperature and pressure studied, the absolute average percentage deviation (AAPD) of the calculated results was determined for each set of mixing rules using eq 5:

$$AAPD = \left(\sum_{i=1}^{n} \frac{\left| y_{2,i} - y_{2,i}^{calcd} \right|}{y_{2,i}} \right) \cdot \frac{(100\ \%)}{n} \quad (5)$$

dx.doi.org/10.1021/je100923d |J. Chem. Eng. Data XXXX, XXX, 000–000

Table 4. Sets of Mixing Rules for the Calculation of the Mixture Parameters a_M and b_M of the Peng−Robinson Equation

	set 1	set 2	set 3
a_{ij}	$a_{ij} = (a_i \cdot a_j)^{1/2} \cdot (1 - k_{ij})$	$a_{ij} = (a_i \cdot a_j)^{1/2} \cdot (1 - k_{ij})$	$a_{ij} = (a_i \cdot a_j)^{1/2} \cdot (1 - k_{ij})$
b_{ij}	$b_{ij} = (b_i + b_j)/2$	$b_{ij} = [(b_i + b_j)/2] \cdot (1 - \delta_{ij})$	$b_{ij} = [(b_i^{1/3} + b_j^{1/3})^3/8] \cdot (1 - \delta_{ij})$
observations	$k_{ij} = k_{ji}$, $k_{ii} = 0$	$k_{ij} = k_{ji}$, $k_{ii} = 0$, $\delta_{ij} = \delta_{ji}$, $\delta_{ii} = 0$	$k_{ij} = k_{ji}$, $k_{ii} = 0$, $\delta_{ij} = \delta_{ji}$, $\delta_{ii} = 0$
refs	39	40, 41	23
	set 4	**set 5**	**set 6**
a_{ij}	$a_{ij} = [(a_i + a_j)/2] \cdot (1 - k_{ij})$	$a_{ij} = (a_i \cdot a_j)^{1/2} \cdot (1 - k_{ij})$	$a_{ij} = (a_i \cdot a_j)^{1/2} \cdot [1 - k_{ij} + (k_{ij} - k_{ji}) \cdot y_i]$
b_{ij}	$b_{ij} = [(b_i + b_j)/2] \cdot (1 - \delta_{ij})$	$b_{ij} = (b_i \cdot b_j)^{1/2} \cdot (1 - \delta_{ij})$	$b_{ij} = (b_i + b_j)/2$
observations	$k_{ij} = k_{ji}$, $k_{ii} = 0$, $\delta_{ij} = \delta_{ji}$, $\delta_{ii} = 0$	$k_{ij} = k_{ji}$, $k_{ii} = 0$, $\delta_{ij} = \delta_{ji}$, $\delta_{ii} = 0$	$k_{ij} \neq k_{ji}$, $k_{ii} = 0$
refs	15	15	41, 42

Table 5. Optimal Values of the Adjustable Parameters for the Calculation of the Mixture Parameters a_M and b_M in the Peng−Robinson Equation and Absolute Average Percentage Deviations (AAPDs) between the Calculated and Experimental Solubility Values for the Different Sets of Mixing Rules Evaluated (Values in Italics for Each Parameter Specify the 95 % Confidence Interval)

mixing rule set	k_{12}		δ_{12}		k_{21}		AAPD/%
1	0.1281	*+0.0038*	−		−		22.09
		−0.0318					
2	0.0370	*+0.0083*	−0.2373	*+0.0587*	−		16.84
		−0.0230		*−0.0252*			
3	0.0379	*+0.0083*	−0.3787	*+0.0657*	−		16.85
		−0.0231		*−0.0281*			
4	0.5519	*+0.0077*	−0.1408	*+0.0327*	−		16.40
		−0.0070		*−0.0581*			
5	0.0371	*+0.0083*	−0.4653	*+0.0694*	−		16.84
		−0.0230		*−0.0299*			
6	−0.5000	*+20.7738*	−		0.1238	*+0.0056*	21.99
		−218.3975				*−0.0334*	

The results obtained from the correlations of the experimental results using the Peng−Robinson equation of state with various sets of mixing rules are shown in Table 5, which summarizes the optimal values of the adjustable parameters (with their corresponding 95 % confidence intervals written in italics) as well as the AAPDs of the calculated solubility values. Before the fitting results are discussed, it should be pointed out that for mixing rule set 6, the optimal value obtained for parameter k_{12} (around −160) had no physical meaning, and for this reason, the optimization method was run with this parameter restricted to values from −0.5 to 0.5. This is probably the reason that the 95 % confidence interval obtained for k_{12} is so wide in that case.

Regarding the fitting accuracy, it can be observed from Table 5 that mixing rule set 1 presented the highest AAPD value (22.1 %) and thus the worst adjustment results, as should be expected since it involves the use of only one adjustable parameter. On the other hand, mixing rule sets 2 to 5 presented smaller values of the AAPD (around 17 %), which can be explained by the fact that two adjustable parameters are used to correct the values of the mixture parameters a_M and b_M. Among these, set 4 yielded the best fit of the experimental results. Lastly, it can be seen that although mixing rule set 6 involves the use of two parameters, its AAPD was similar to that obtained with set 1. Therefore, for the case studied (the solubility of 9*H*-carbazole in propane), the use of set 6 is not recommended. Nevertheless, it should be noted that the differences between results predicted by the different sets of mixing rules were not statistically significant (with 95 % probability), as inferred from null-hypothesis significance testing.[43]

Finally, a sensitivity analysis of the models (Peng−Robinson equation with different sets of mixing rules) was performed by varying the values of the fitted parameters by ± 10 %. In the case of set 1, variation of the fitting parameter k_{12} by ± 10 % caused increases of less than 9 % in the AAPD. For sets 2, 3, and 5, variation of the fitting parameters k_{12} and δ_{12} produced similar results: weak sensitivity of the models to the value of k_{12} (variations of ± 10 % led to increases in AAPD smaller than 1.5 %) and a strong sensitivity to the value of δ_{12} [variations of ± 10 % produced AAPD increases between (5 and 12) %]. In the case of set 4, the model predictions were strongly related to the value of k_{12} [variations of (−10 and +10) % in this parameter led to variations of (600 and 80) %, respectively, in the AAPD value] but showed a very weak sensitivity to the value of the other parameter, δ_{12}. For set 6, it was found that the model predictions were not dependent on the variation of the parameter k_{12} by ± 10 %. This observation is probably related to the wide confidence interval of the parameter, as mentioned above. On the contrary, the model was sensitive to k_{21}, as the AAPD increased by about 9 % when the parameter was varied by ± 10 %.

To give a visual idea of the correlation of the experimental results obtained using the Peng−Robinson equation with mixing rule set 4, Figure 4 compares the experimental and calculated values of the mole fraction of 9*H*-carbazole. Generally good agreement between the experimental and calculated results can

dx.doi.org/10.1021/je100923d |*J. Chem. Eng. Data* XXXX, XXX, 000–000

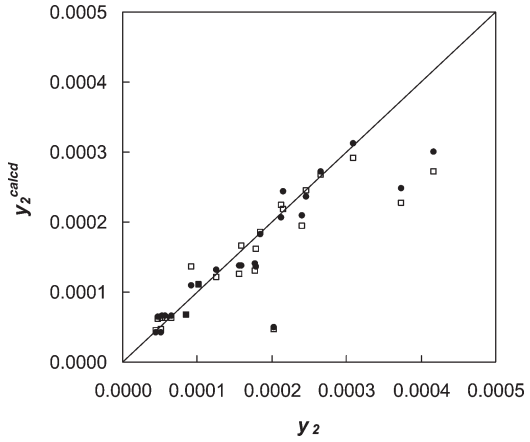

Figure 4. Comparison of the experimental solubility data (y_2) with calculated values (y_2^{calcd}) obtained from the Peng−Robinson equation using mixing rule 4 and from the Chrastil equation: ●, Peng−Robinson equation; □, Chrastil equation.

Table 6. Optimal Values of the Adjustable Parameters Obtained from the Correlation of the Experimental Data with the Chrastil Equation and the AAPD between the Experimental and Calculated Data (Values in Italics for Each Parameter Specify the 95 % Confidence Interval)

a_0	−7.090	*+0.496*
		−0.095
a_1	−5180.001	*+181.225*
		−37.278
a_2	2.125	*+0.082*
		−0.018
AAPD/%	16.56	

be observed. It should be mentioned, however, that the parameters were obtained by fitting of solubility data, which may present limitations in the simulation of enthalpies or densities.

3.2. Data Correlation: Chrastil Equation. The Chrastil model relates the solubility of a solute (y_2) in a fluid at high pressure to the density of the fluid (ρ) and the temperature (T) as shown in eq 6:[44]

$$\ln y_2 = a_0 + \frac{a_1}{T} + a_2 \cdot \ln \rho \qquad (6)$$

where a_0, a_1, and a_2 are adjustable parameters. Despite the simplicity of this equation, it is often used because it provides good correlations of experimental data. In this work, values of the parameters were calculated by minimizing the OBF (eq 4), which compares the experimental (y_2) and calculated (y_2^{calcd}) values of the mole fraction of 9*H*-carbazole. Table 6 summarizes the values of the optimal adjustable parameters and the AAPD obtained from the correlation of the experimental data using the Chrastil equation (together with the 95 % confidence intervals for the adjustable parameters). It can be observed that the value of the AAPD is very close to that obtained using the Peng−Robinson equation of state. Nevertheless, it should be noted that the Chrastil model requires the use of three adjustable parameters, as opposed to the two adjustable parameters involved in the correlation with the Peng−Robinson equation. A graphical comparison of the experimental data and the values of solubility predicted by the Chrastil equation is given in Figure 4. Good agreement between the experimental and estimated data can be observed.

Finally, a sensitivity analysis of the Chrastil model was carried out by varying the values of the fitting parameters a_0, a_1, and a_2 by ± 10 %. It was observed that the model predictions were strongly dependent on the fitted parameters. Thus, variations of the parameters by ± 10 % produced increases larger than 35 % in the AAPD values.

CONCLUSIONS

The solubility of 9*H*-carbazole in propane has been measured by a static method at temperatures from (323 to 405) K and pressures in the range (4.3 to 10.0) MPa. The values of the mole fraction of 9*H*-carbazole varies from $4 \cdot 10^{-5}$ to $4 \cdot 10^{-4}$ over the range of experimental conditions studied. The solubilities of 9*H*-carbazole in propane are 1 order of magnitude larger than those of 9*H*-carbazole in carbon dioxide (as reported in the literature) for similar values of the reduced pressure and temperature. This fact is indicative of the excellent solvent properties of propane relative to CO_2 (the SCF solvent most commonly employed) for use in either supercritical reactions or supercritical extractions involving 9*H*-carbazole, the chemical species used in this work as representative of the PAH family of compounds. The solubility data were modeled using the Peng−Robinson equation of state, and six different sets of mixing rules were evaluated; good agreement of the results was obtained using sets of mixing rules involving two adjustable parameters (AAPD of 16.4 % for the best fit). Likewise, the empirical model of Chrastil (which involves three parameters) was used to correlate the experimental data and also yielded good agreement between the experimental and modeled results (AAPD of 16.6 %). These results point out that the mathematical equations proposed (the Peng−Robinson equation of state and the Chrastil equation) can be used to predict the solubility of 9*H*-carbazole in propane fairly accurately.

AUTHOR INFORMATION

Corresponding Author

*Tel.: +34 902204100. Fax: +34 925268840. E-mail: jesusa.rincon@uclm.es.

Funding Sources

The authors gratefully acknowledge the MMAM and MCyT of Spain and the Junta de Comunidades de CLM for financial support of this work through Projects 096/2006/3-11.3, A141/2007/2-11.3, CMT 2006-10105, and PAI08-0195-3614.

REFERENCES

(1) Liu, T.; Li, S.; Zhou, R.; Jia, D.; Tian, S. Solubility of Triphenylmethyl Chloride and Triphenyltin Chloride in Supercritical Carbon Dioxide. *J. Chem. Eng. Data* **2009**, *54*, 1913–1915.

(2) Zhang, G.; Cui, Z.; Ling, J. Supercritical CO_2 Extraction of PAHs from Contaminated Soil Treated by a Composting Method. *J. Liq. Chromatogr. Relat. Technol.* **2008**, *31*, 695–701.

(3) Anitescu, G.; Tavlarides, L. L. Supercritical Extraction of Contaminants from Soils and Sediments. *J. Supercrit. Fluids* **2006**, *38*, 167–180.

(4) Vradman, L.; Herskowitz, M.; Korin, E.; Wisniak, J. Regeneration of Poisoned Nickel Catalyst by Supercritical CO_2 Extraction. *Ind. Eng. Chem. Res.* **2001**, *40*, 1589–1590.

(5) Clark, M. C.; Subramaniam, B. Extended Alkylate Production Activity during Fixed-Bed Supercritical 1-Butene/Isobutane Alkylation on Solid Acid Catalysts Using Carbon Dioxide as a Diluent. *Ind. Eng. Chem. Res.* **1998**, *37*, 1243–1250.

(6) Subramanian, B. Enhancing the Stability of Porous Catalysts with Supercritical Reaction Media. *Appl. Catal., A* **2001**, *212*, 199–213.
(7) Chen, G. M.; Zhang, X. W.; Mi, Z. T. Effects of Pressure on Coke and Formation of Its Precursors during Catalytic Cracking of Toluene over USY Catalyst. *J. Fuel Chem. Technol.* **2007**, *35*, 211–216.
(8) Rodríguez, A.; Uguina, M. A.; Capilla, D.; Pérez-Velazquez, A. Effect of Supercritical Conditions on the Transalkylation of Diethylbenzene with Benzene. *J. Supercrit. Fluids* **2008**, *46*, 57–62.
(9) Kozhevnikov, I. V. Heterogeneous Acid Catalysis by Heteropoly Acids: Approaches to Catalyst Deactivation. *J. Mol. Catal. A: Chem.* **2009**, *305*, 104–111.
(10) Yang, H.; Zhong, C. Modeling of the Solubility of Aromatic Compounds in Supercritical Carbon Dioxide−Cosolvent Systems Using SAFT Equation of State. *J. Supercrit. Fluids* **2005**, *33*, 99–106.
(11) García-González, J.; Molina, M. J.; Rodríguez, F.; Mirada, F. Solubilities of Phenol and Pyrocatechol in Supercritical Carbon Dioxide. *J. Chem. Eng. Data* **2001**, *46*, 918–921.
(12) Yamini, Y.; Bahramifar, N. Solubility of Polycyclic Aromatic Hydrocarbons in Supercritical Carbon Dioxide. *J. Chem. Eng. Data* **2000**, *45*, 53–56.
(13) Macnaughton, S. J.; Kikic, I.; Rovedo, G.; Foster, N. R.; Alessi, P. Solubility of Chlorinated Pesticides in Supercritical Carbon Dioxide. *J. Chem. Eng. Data* **1995**, *40*, 593–597.
(14) Miller, D. J.; Hawthorne, S. B. Solubility of Polycyclic Aromatic Hydrocarbons in Supercritical Carbon Dioxide from 313 K to 523 K and Pressures from 100 bar to 450 bar. *J. Chem. Eng. Data* **1996**, *41*, 779–786.
(15) Martínez, F.; Martín, A.; Asencio, I.; Rincón, J. Solubility of Anthracene in Sub- and Supercritical Propane. *J. Chem. Eng. Data* **2010**, *55*, 1232–1236.
(16) Ahlers, J.; Yamaguchi, T.; Gmehling, J. Development of a Universal Group Contribution Equation of State. 5. Prediction of the Solubility of High-Boiling Compounds in Supercritical Gases with the Group Contribution Equation of State Volume-Translated Peng−Robinson. *Ind. Eng. Chem. Res.* **2004**, *43*, 6569–6576.
(17) Iwai, Y.; Uchida, H.; Arai, Y.; Mori, Y. Monte Carlo Simulation of Solubilities of Naphthalene, Phenanthrene, and Anthracene in Supercritical Fluids. *Fluid Phase Equilib.* **1998**, *144*, 233–244.
(18) Kalaga, A.; Trebble, M. Solubilities of Tetracosane, Octacosane, and Dotriacontane in Supercritical Ethane. *J. Chem. Eng. Data* **1997**, *42*, 368–370.
(19) Kurnik, R. T.; Reid, R. C. Solubility of Solid Mixtures in Supercritical Fluids. *Fluid Phase Equilib.* **1982**, *8*, 93–105.
(20) Kurnik, R. T.; Holla, S. J.; Reid, R. C. Solubility of Solids in Supercritical Carbon Dioxide and Ethylene. *J. Chem. Eng. Data* **1981**, *26*, 47–51 .
(21) Rincón, J.; Cañizares, P.; García, M. T. Improvement of the Waste-Oil Vacuum-Distillation Recycling by Continuous Extraction with Dense Propane. *Ind. Eng. Chem. Res.* **2007**, *46*, 266–272.
(22) Rincón, J.; Cañizares, P.; García, M. T.; Gracia, I. Regeneration of Used Lubricant Oil by Propane Extraction. *Ind. Eng. Chem. Res.* **2003**, *42*, 4867–4873.
(23) Goodarznia, I.; Esmaeilzadeh, F. Solubility of an Anthracene, Phenanthrene, and Cabazol Mixture in Supercritical Carbon Dioxide. *J. Chem. Eng. Data* **2002**, *47*, 333–338.
(24) Lemmon, E. W.; McLinden, M. O.; Friend, D. G. Thermophysical Properties of Fluid Systems. *NIST Chemistry WebBook, NIST Standard Reference Database Number 69*; Linstrom, P. J., Mallard, W. G., Eds.; National Institute of Standards and Technology: Gaithersburg, MD, 2005; http://webbook.nist.gov.
(25) Streng, A. G. Miscibility and Compatibility of Some Liquid and Solidified Gases at Low Temperature. *J. Chem. Eng. Data* **1971**, *16*, 357–359.
(26) Majer, V.; Svoboda, V. *Enthalpies of Vaporization of Organic Compounds: A Critical Review and Data Compilation*; Blackwell Scientific Publications: Oxford, England, 1985.
(27) Mushrif, S. H.; Phoenix, A. V. Effect of Peng−Robinson Binary Interaction Parameters on the Predicted Multiphase Behavior of Selected Binary Systems. *Ind. Eng. Chem. Res.* **2008**, *47*, 6280–6288.
(28) Yaws, C. L. *Chemical Properties Handbook*; McGraw Hill: New York, 1999.
(29) Weast, R. C.; Grasselli, J. G. *CRC Handbook of Data on Organic Compounds*, 2nd ed.; CRC Press: Boca Raton, FL, 1989.
(30) Sivaraman, A.; Martin, R. J.; Kobayashi, R. A Versatile Apparatus To Study the Vapor Pressures and Heats of Vaporization of Carbazole, 9-Fluorenone and 9-Hydroxyfluorene at Elevated Temperatures. *Fluid Phase Equilib.* **1983**, *12*, 175–188.
(31) Coplen, T. B.; Böhlke, J. K.; De Bièvre, P.; Ding, T.; Holden, N. E.; Hopple, J. A.; Krouse, H. R.; Lamberty, A.; Peiser, H. S.; Revesz, K.; Rieder, S. E.; Rosman, K. J. R.; Roth, E.; Taylor, P. D. P.; Vocke, R. D.; Xiao, Y. K. Isotope-Abundance Variations of Selected Elements (IUPAC Technical Report). *Pure Appl. Chem.* **2002**, *74*, 1987–2017.
(32) Jimenez, P.; Roux, M. V.; Turrión, C. Thermochemical Properties of N-Heterocyclic Compounds III. Enthalpies of Combustion, Vapour Pressures and Enthalpies of Sublimation, and Enthalpies of Formation of 9*H*-Carbazole, 9-Methylcarbazole, and 9-Ethylcarbazole. *J. Chem. Thermodyn.* **1990**, *22*, 121–726.
(33) Miyamoto, H.; Watanabe, K. A Thermodynamic Property Model for Fluid-Phase Propane. *Int. J. Thermophys.* **2000**, *21*, 1045–1072.
(34) *Quantifying Uncertainty in Analytical Measurement*, 2nd ed.; Ellison, S. L. R., Rosslein, M., Williams, A., Eds.; EURACHEM/CITAC Guide 4, 2000.
(35) Taylor, B. N.; Kuyatt, C. E. *Guidelines for Evaluating and Expressing the Uncertainty of NIST Measurement Results*; NIST Technical Note 1297; National Institute of Standards and Technology: Gaithersburg, MD, 1994.
(36) Stahl, E.; Quirin, K. W.; Gerard, D. *Dense Gases for Extraction and Refining*; Springer-Verlag: Berlin, 1988.
(37) Clifford, T. *Fundamentals of Supercritical Fluids*; Oxford University Press: New York, 1999.
(38) Radomska, M.; Radomski, R. Calorimetric Studies of Binary Systems of 1,3,5-Trinitrobenzene with Naphthalene, Anthracene and Carbazole. II. Phase Diagrams. *Thermochim. Acta* **1980**, *40*, 415–425.
(39) Peng, D. Y.; Robinson, D. B. A New Two-Constant Equation of State. *Ind. Eng. Chem. Fundam.* **1976**, *15*, 59–64.
(40) Pérez, E.; Cabañas, A.; Sánchez-Vicente, Y.; Renuncio, J. A. R.; Pando, C. High-Pressure Phase Equilibria for the Binary System Carbon Dioxide + Dibenzofuran. *J. Supercrit. Fluids* **2008**, *46*, 238–244.
(41) Shibata, S. K.; Sandler, S. I. Critical Evaluation of Equation of State Mixing Rules for the Prediction of High-Pressure Phase Equilibria. *Ind. Eng. Chem. Res.* **1989**, *28*, 1893–1898.
(42) Panagiotopoulos, A. Z.; Reid, R. L. High-Pressure Phase Equilibria in Ternary Fluid Mixtures with Supercritical Component. In *Supercritical Fluids: Chemical and Engineering Principles and Applications*; Squire, T. G., Paulaitis, M. E., Eds.; ACS Symposium Series 329; American Chemical Society: Washington, DC, 1987; pp 115−129.
(43) Triola, M. F. *Elementary Statistics*, 11th ed.; Addison Wesley Longman: New York, 2008.
(44) Chrastil, J. Solubility of Solids and Liquids in Supercritical Gases. *J. Phys. Chem.* **1982**, *86*, 3016–3021.